Mem. S.A.It. Vol. 78, 278

Memorie della

Resolving stellar surface spots

K. G. Strassmeier[1], T. Carroll[1], J. B. Rice[2] and I. S. Savanov[1]

[1] Astrophysical Institute Potsdam (AIP), An der Sternwarte 16, D-14482 Potsdam, Germany e-mail: kstrassmeier@aip.de
[2] Department of Physics, Brandon University, Brandon, Manitoba R7A 6A9, Canada

Abstract. Doppler imaging of stellar surfaces is a novel technique with similarities to medical brain tomography (instead of a fixed brain and a rotating scanner, astronomers have a fixed spectrograph and a rotating brain, star of course). The number of free (internal) parameters is of the order of the number of surface grid points and only constrained by the number of input data points. This obviously ill-posed situation requires modern inversion algorithms with penalty functions of the form of maximum entropy or Tikhonov etc.. We present a brief status review of our Doppler imaging codes at AIP that span from temperature and spot-filling-factor mapping to full Stokes-based magnetic field mapping.

Key words. stars: activity of – starspots – stars: imaging – stars: magnetic fields – stars: late-type

1. Introduction

The atmospheres of magnetically-active cool stars are known to exhibit most, if not all, features of the active Sun. Firstly, these atmospheres seem to consist also of a photosphere, a chromosphere, and an outer corona with its respective and distinct spectral fingerprints. Secondly, a variety of magnetic activity tracers are observed on such stars, e.g. cool spots, flares, and hot plages (see, e.g., the review by Schrijver (2002)). These are usually observed on a much enhanced flux and geometric scale compared to the Sun but are thought to be associated with similar events like rising magnetic-flux tubes, enhanced ultraviolet and X-ray emission due to coronal heating, and long-term light variability due to magnetic cycles.

Doppler imaging is an observational and computational technique similar to tomography wherein a series of high-resolution spectral line profiles are inverted into an "image" of the stellar surface. Complex computer codes were developed over the recent years. Our own codes are TempMap originally by Rice et al. (1989) for magnetic Ap stars and extended to cool stars by Rice & Strassmeier (2000) and Rice (2002), OPC by Savanov & Strassmeier (2005) for mapping very cool stars from molecular lines, and *iMap* by Kopf et al. (2006) for Zeeman mapping from full Stokes-profiles. TempMap was applied to spectral-line data for numerous active late-type stars in a series of papers in A&A (most recently by Strassmeier & Rice ((2006), see Fig. 1) while the other codes have not yet seen real starlight, at least not in the literature.

Send offprint requests to: K. G. Strassmeier

2. How does Doppler imaging work?

The cool version of TempMap recovers the surface temperature distribution from the integral equation that relates the distribution of surface temperature to the observed line profile and light curve variations. Local line profiles are computed from a numerical solution of the equation of transfer with 72 depth points from the grid of model atmospheres published by Kurucz (1993). These model atmospheres are precalculated assuming LTE. The local line profile for each small surface segment is obtained from the grid of profiles by interpolation to match the local effective temperature.

The effects of noise in the data are controlled by a penalty function, or regularizing functional, that prevents the overinterpretation of information contained in the line profiles and the light curve. TempMap incorporates a choice between using a maximum entropy penalty function in solving the inverse problem, or using a Tikhonov penalty function. The form taken by the maximum entropy penalty function is

$$f_{en} = \sum_i F_i \ln(F_i). \quad (1)$$

Here F is approximated by ωT^4 with ω as an arbitrary constant and T as the local effective temperature normalized by the average effective temperature over the surface of the star. The Tikhonov penalty function is usually represented as

$$f_t = \int_{-\pi}^{\pi} \int_{-\pi/2}^{\pi/2} [(\frac{\partial \tau}{\partial \phi})^2 + (\frac{\partial \tau}{\partial l})^2] d\phi dl \quad (2)$$

where ϕ represents latitude on the stellar surface and l is a linearized measure of longitude (see Piskunov & Rice (1993)). In practice, the choice between these has little significance because normally only small weighting is given to the penalty function when the noise problem is not serious. Overall, Rice & Strassmeier (2000) concluded that S/N ratio *alone* does not significantly improve the image recovery once S/N≈300:1 is surpassed if all other factors are perfect. This strips down to knowing and treating the systematic noise in a spectrum.

Nowadays, we proceed with the inversion of a wavelength range of size of roughly one echelle order. Each rotational phase then consists of a data vector of length typically 3000 wavelength points, or 5.5 nm, and typically 20–60 phases, e.g., for PW And and σ^2 CrB; Strassmeier & Rice (2006), (2003). This vector contains the major mapping lines (up to 10) plus a total of 51 blends and indirectly is equivalent to increased S/N ratio per line.

Another approach to increase the S/N ratio is "least-squares deconvolution". It allows to reconstruct a single high signal-to-noise line profile from all spectral lines contained in a spectrum and thereby bypassing the stringent S/N constrain for Doppler imaging. This requires the knowledge of the basic parameters of the stellar atmosphere in order to calculate a synthetic spectrum to be used as a template for the deconvolution, or uses observed template spectra of appropriate inactive stars. The method has been developed and successfully applied by Donati et al. (1997). See the contributions by M. Jardine and B. Marsden in these proceedings.

The surface Doppler-shift constraint from the stellar rotation restricts the freedom of the surface grid points so that we are left with only ten parameters that are in any sense mathematically free ($\log g$, $T_{\rm phot}$, $v_{\rm e} \sin i$, Inclination i, Microturbulence, Macroturbulence, Abundance, plus three atomic parameters; $\log gf$, damping, and central wavelength). Yet these ten parameters are still not completely independent or free of physical constraint. For example if $v_{\rm eq} \sin i$ is measured and i fixed, $v_{\rm eq}$ is no longer a free parameter. The same is true if we fixed the gravity and the line strength, then the microturbulence is no longer completely free because the equivalent width must be reproduced. This shrinks our problem basically to the common range of uncertainties of stellar astrophysical parameters and atomic line data.

Rice & Strassmeier (2000) visualized the quantitative influence of the uncertainties of many of the stellar quantities and atomic data. We demonstrated the extreme robustness of Doppler imaging to even exaggerated assumptions, e.g. a recovery with a phase gap of

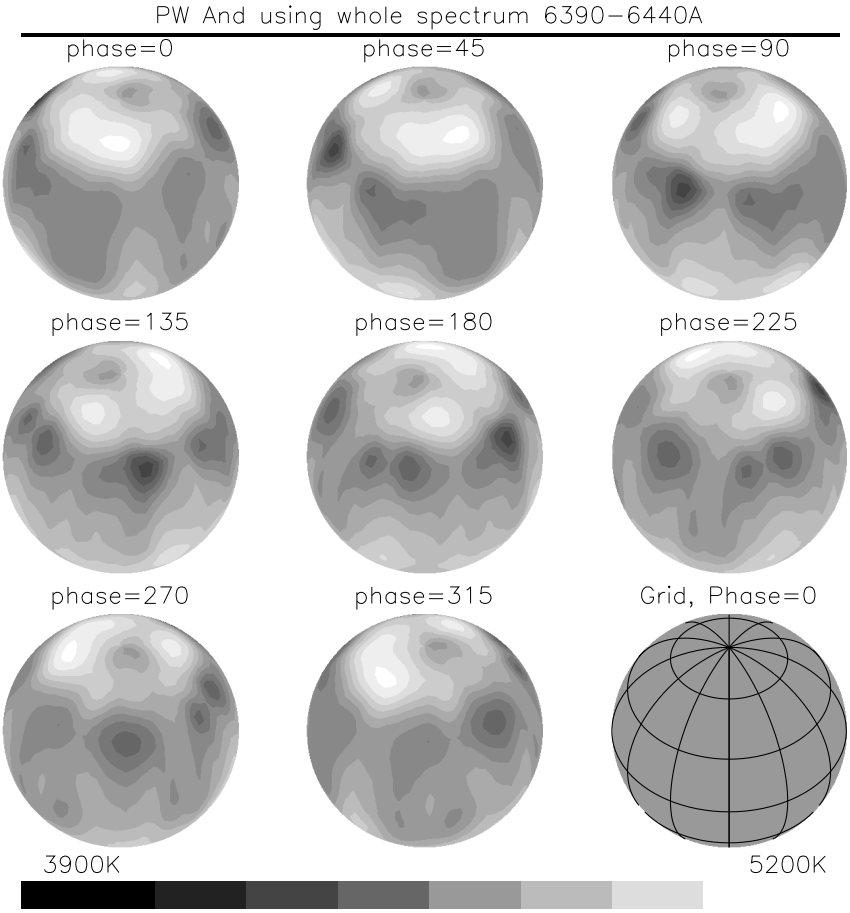

Fig. 1. Doppler image of PW And (K2 ZAMS) from a full-spectrum approach. Temperature maps are plotted in a spherical projection at eight equidistant rotational phases. The temperature scale is indicated and is the same for all projections. The image is a simultaneous reconstruction from 10 spectral lines with 51 blends, see text. Note that the photospheric temperature is ≈5,000 K.

100° (0.28) with moderate S/N still correctly recovered the spots located within the phase gap. Having simultaneous photometry in two bandpasses not only gave a better handle on the overall temperature of the stellar surface but when used with the line equivalent width the photometry provided a powerful additional constraint so that we are forced to make adjustments in factors such as element abundance to compensate for uncertainty in atomic parameters or $\log g$. This works to minimize the impact on the recovered image when errors in adopted line parameters such as the damping constants occur.

A recent extension to Doppler imaging of optically-thin (atomic) lines is the use of molecular bands and bandheads. Stars cooler than, say, M2 could only be mapped by considering the many molecular bands because the thermal energy is too small to populate the higher atomic levels and also because more atoms are being bound in molecules and are missing for the atomic line formation. Savanov & Strassmeier (2005) presented a new Doppler-imaging inversion code that uses

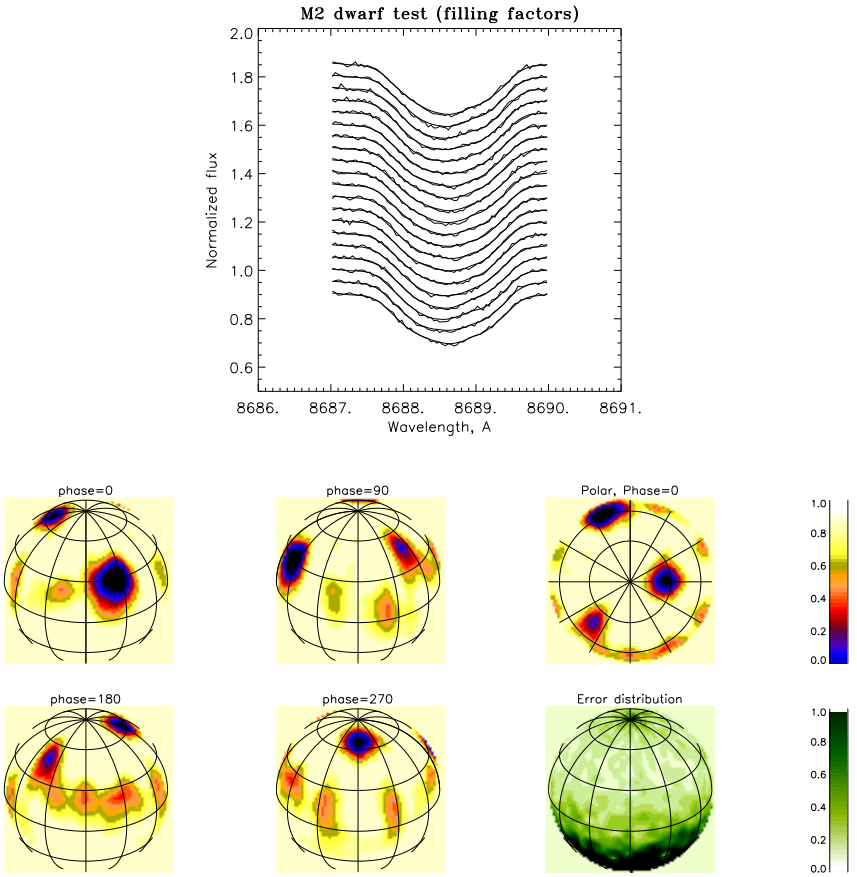

Fig. 2. Test inversion from an artificial M2 star ($T_{\rm eff}$= 3500 K, log g=5.0) using "filling factor" as the inversion parameter. One atomic line (Fe I868.862nm) and many molecular lines, mostly CN, were used. Thin lines in the top panel are the artificial data, the thick lines are the reconstruction with object's principal components. The lower panels shows the reconstructed image.

quasi-optimal filtering of the object's principal components of a Fisher information matrix, based on an approach developed by Terebizh (2004). The new code allows to perform the reconstruction of stellar surface temperature maps using molecular features like TiO, CO, OH, CN etc. which are numerous in spectra of late-type stars. According to this approach the linear Doppler-imaging transformation is a matrix problem of the form

$$y_0 = Hx_0 + \xi, \qquad (3)$$

where the $n \times 1$-vector x_0 is an unknown object, the $m \times n$-matrix H is the point spread function, ξ is random noise, and the $m \times 1$-vector y_0 is the observed image. To reduce the number m of dimension of the vector that describes the misfit between the observed image and its estimate to number n, a simple procedure based on single-value decomposition is used. We can then define a vector of the object principal components and the corresponding vector of the least-squares estimate principal components to linearize the problem. Like the familiar Fourier coefficients the principal

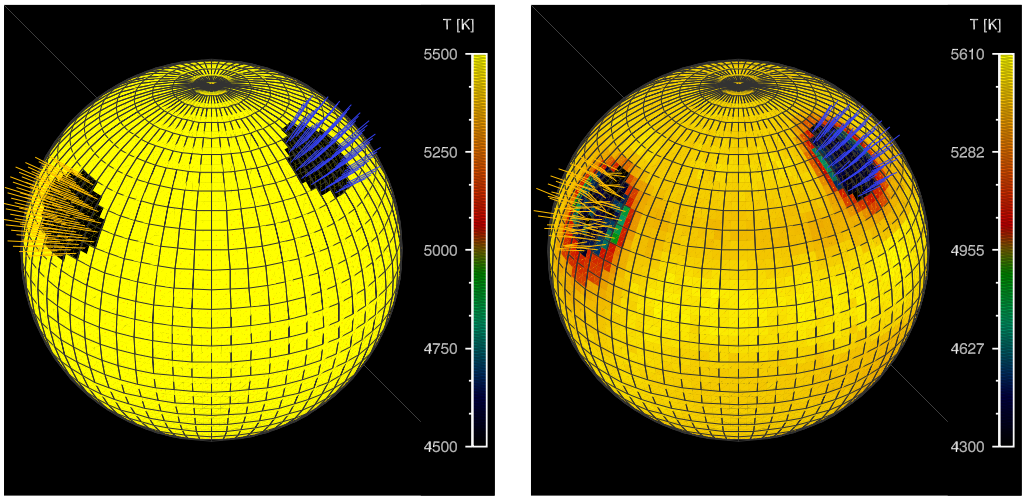

Fig. 3. Artificial test star (left) and its recovered image by *iMap* (right). The test star has a bipolar spot configuration with a radial field strength of +1500 G (left spot) and −1500 G (right spot).

components are often easier to recover than the object itself. The squared error of the filtered estimate can be minimized by a set of weights which constitute the optimal Wiener filter.

Fig. 2 is a test inversion from an artificial M2V star. The method produces stable and efficient solutions by relying only on the internal resources of the inverse theory, namely on the assumption about the structure of the optimal estimate. Non-monotonic behavior of the quasi-optimal filter is different than from the one for the truncated estimate (e.g. Berdyugina (1998)). The quasi-optimal filter leaves in the object's estimate only those principal components that have the highest accuracy of restoration.

One of our central scientific objectives of our research is to find and interpret observational evidence for stellar dynamos. Especially in the context of our upcoming PEPSI instrument at the LBT (Strassmeier et al. (2004)), we need to interpret high-resolution Stokes IQUV spectra of solar-type stars. We have therefore developed a Zeeman-Doppler imaging (ZDI) code to allow simultaneous temperature and magnetic field inversion by means of a spectral decomposition technique and artificial neural networks. Kopf, Carroll & Strassmeier (2006) presented a first demonstration of the code nicknamed *iMap* (Kopf, PhD-thesis). As a first step, local Stokes line profiles are decomposed into their respective eigenspectra via a Principle Component Analysis (PCA). A set of Multi Layer Perceptrons (MLP's) is then trained to calculate the reduced eigenspectrum of local Stokes profiles as a function of the line of sight angle, effective temperature of the underlying model atmosphere, and the magnetic-field configuration. The back transformation gives then the Stokes profiles. The basis of the forward module is the numerical integration of the polarized radiative transfer equation with the quadratic DELO method. The inverse module incorporates an entropy regularized conjugated gradient and a Levenberg-Marquardt method. Our ZDI code simultaneously recovers temperature and magnetic-field distribution from all four Stokes parameters.

To assess the reliability of the inversion, an artificial test star with a bipolar spot group was modelled (Fig. 3, left panel). The spot temperatures were set to 4,500 K, the photosphere at 5,500 K. The magnetic field in each spot was assumed to be radial with a field strength of +1,500 G and −1,500 G, respectively. "Observed" Stokes profiles were calculated for the spectral lines Ca I 6439 and Fe I 6173 for 18 equidistant phases. $V \sin i$ was

set to 35 km s^{-1} with an inclination of 60°. No noise was added to the data. An initial DI run identifies the possible locations of magnetic regions before the actual ZDI is started with the field vectors and the temperature as free parameter. The test inversion had a 3°×3° surface resolution.

The magnetic field topology and temperature distribution of the original image was very well recovered (right panel in Fig. 3). Local and integrated line profiles proved to be remarkably accurate (mean relative rms of 0.17% in Stokes V and better than 2% in Stokes Q&U). The impressive speed of the full Stokes calculation (a factor 1000 faster as with conventional solvers) makes ZDI over a large wavelength range feasible.

3. Discussion

Direct and indirect observations suggest that surface magnetic fields are ubiquitous in *cool stars*. Although not yet fully understood, a dynamo mechanism comparable to the Sun's converts mechanical energy into magnetic flux and transports it up to the surface where it is observable as highly variable spots, plages, flares etc.. It was proposed that the shear beneath the bottom of the convection zone generates an interface dynamo that attempts to couple the two zones, e.g. Charbonneau & MacGregor (1993).

Stars on the upper main sequence present a different picture. Here we encounter large-scale and very stable fields but approximately an order of magnitude higher in strength than on cool stars. The origin of it is likely fossil, i.e. it is a remnant of a field present during an earlier stage of stellar evolution. It is not clear whether the spread of magnetic field strength of a particular group of stars could also be related to the amount of magnetic flux frozen-in during star formation.

On the low-mass end of the ZAMS, Mullan & MacDonald (2001) suggested that even a M6 star should still have a radiative core and therefore an interface-dynamo component. At the spectral type of K2 of a typical active star and a mass of ≈0.8 $M_\odot$, we would expect the interface component still to dominate. Furthermore, as suggested by Mackay et al. (2004), the values for surface meridional flow must be increased by around a factor of 10 to ≈100 m s^{-1} in order to produce magnetic flux at high latitudes, which then would make truly equatorial spots even less likely. Donati et al. (2006) had recently mapped a rapidly-rotating M4-star from atomic Stokes-V profiles and found a very distinctive large-scale polar magnetic field possibly indicative of a distributed-type of dynamo rather than an interface dynamo.

Once stellar models incorporate magneto-convection, stellar evolutionary tracks may become distinctively different. Mullan & MacDonald (2001) found that for two stars with the same mass (valid for masses up to 0.6 $M_\odot$), the magnetic star has a larger radius and a smaller effective temperature than the non-magnetic star. So far, we can not quantify this for very young stars with masses above 0.6 $M_\odot$. However, Ambruster et al. (2003) speculate that the active, Pleiades-age K dwarfs are actually more massive than their spectral classes indicate. If so, our interior models used to host the flux tube emergence (c.f. Granzer et al. (2000)) may be inappropriate as well and, more importantly, the flux tube's starting points in the super-adiabatic layer would be wrong in the first place. We speculate that this could have a dramatic impact for the predicted surface latitudes of flux-tube emergence.

Acknowledgements. KGS thanks Maria Massi and Thomas Preibisch from MPIfR for their kind hospitality. Moira Jardine, Svetlana Berdyugina and Volkmar Holzwarth are thanked for several discussions during the meeting. We thank Markus Kopf for his cool poster.

References

Ambruster, C. W., Fekel, F. C., Brown, A. 2003, in Brown A., Harper G., Ayres T. (eds.), 12th Cool Stars, Stellar Systems, and the Sun, Univ. of Colorado, p.912

Berdyugina, S. 1998, A&A 338, 97

Charbonneau, P., MacGregor, K. B. 1993, ApJ 417, 762

Donati, J.-F., Forveille, T., Cameron, A., et al. 2006, Science 311, 633
Donati, J.-F., Semel, M., Carter, B., Rees, D. E., Collier Cameron, A. 1997, MNRAS 291, 658
Granzer, T., Caligari, P., Schüssler, M., Strassmeier, K. G. 2000, A&A 355, 1087
Kopf, M., Carroll, T., Strassmeier, K. G. 2006, in 14th Cool Stars, Stellar Systems, and the Sun, Pasadena, in press
Kurucz, R. L. 1993, ATLAS-9, CD-ROM #13
Mackay,D. H., Jardine, M., Collier Cameron, A., Donati, J.-F., Hussain, G. A. J. 2004, MNRAS 354, 737
Mullan, D. J., MacDonald, J. 2001, ApJ 559, 353
Piskunov, N. E., Rice, J. B. 1993, PASP 105, 1415
Rice, J. B. 2002, AN 323, 220
Rice, J. B., Strassmeier, K. G. 2000, A&AS 147, 151
Rice J. B., Wehlau W. H., Khokhlova V. L., 1989, A&A 208, 179
Savanov, I., Strassmeier, K. G. 2005, A&A 444, 931
Schrijver, C. J. 2002, AN 323, 157
Strassmeier, K. G., Pallavicini, R., Rice, J. B., Andersen, M. I., Zerbi, F. M. 2004, AN 325, 278
Strassmeier, K. G., Rice, J. B. 2003, A&A 399, 315
Strassmeier, K. G., Rice, J. B. 2006, A&A 460, 751
Terebizh, V. Y. 2004, A&A Trans. 23, 85